Title: Epidemiological modeling of SARS-CoV-2 in white-tailed deer (*Odocoileus virginianus*) reveals conditions for introduction and widespread transmission.

Running title: SARS-CoV-2 outbreaks in white-tailed deer

PROPOSED AUTHOR LIST: ELIAS ROSENBLATT[1, *], JONATHAN D. COOK[2], GRAZIELLA V. DIRENZO[3,4], EVAN H.C. GRANT[5], FERNANDO ARCE [4], KIM M. PEPIN[6], F. JAVIERA RUDOLPH[2,7], MICHAEL C. RUNGE[2], SUSAN SHRINER[6], DANIEL P. WALSH[8], BRITTANY A. MOSHER[1]

[1] *Rubenstein School of Environment and Natural Resources, University of Vermont, Burlington, VT, USA*

[2] *U.S. Geological Survey, Eastern Ecological Science Center, Laurel, MD, USA*

[3] *U. S. Geological Survey, Massachusetts Cooperative Fish and Wildlife Research Unit, University of Massachusetts, Amherst, MA, USA*

[4] *Department of Environmental Conservation, University of Massachusetts, Amherst, MA, USA*

[5] *U.S. Geological Survey, Eastern Ecological Science Center, Turner's Falls, MA, USA*

[6] *National Wildlife Research Center, USDA, APHIS, Fort Collins, CO, USA*

[7] *Department of Ecosystem Sciences and Management, Pennsylvania State University, University Park, PA, USA*

[8] *U. S. Geological Survey, Montana Cooperative Wildlife Research Unit, University of Montana, Missoula, MT, USA*

[*] *Correspondence: Elias Rosenblatt, Email: erosenbl@uvm.edu*

Abstract

Emerging infectious diseases with zoonotic potential often have complex socioecological dynamics and limited ecological data, requiring integration of epidemiological modeling with surveillance. Although our understanding of SARS-CoV-2 has advanced considerably since its detection in late 2019, the factors influencing its introduction and transmission in wildlife hosts, particularly white-tailed deer (*Odocoileus virginianus*), remain poorly understood. We use a Susceptible-Infected-Recovered-Susceptible epidemiological model to investigate the spillover risk and transmission dynamics of SARS-CoV-2 in wild and captive white-tailed deer populations across various simulated scenarios. We found that captive scenarios pose a higher risk of SARS-CoV-2 introduction from humans into deer herds and subsequent transmission among deer, compared to wild herds. However, even in wild herds, the transmission risk is often substantial enough to sustain infections. Furthermore, we demonstrate that the strength of introduction from humans influences outbreak characteristics only to a certain extent. Transmission among deer was frequently sufficient for widespread outbreaks in deer populations, regardless of the initial level of introduction. We also explore the potential for fence line interactions between captive and wild deer to elevate outbreak metrics in wild herds that have the lowest risk of introduction and sustained transmission. Our results indicate that SARS-CoV-2 could be introduced and maintained in deer herds across a range of circumstances based on testing a range of introduction and transmission risks in various captive and wild scenarios. Our approach and findings will aid One Health strategies that mitigate persistent SARS-CoV-2 outbreaks in white-tailed deer populations and potential spillback to humans.

Keywords: SARS-CoV-2; zoonotic disease; SIR; white-tailed deer, outbreak

1. Introduction

Many emerging infectious diseases in animal populations are transmissible to humans, representing a public health threat (Taylor et al. 2001; Rahman et al. 2020). These diseases are called zoonoses and pose One Health challenges, meaning closely linked human, animal, and ecosystem health challenges that often require coordinated, multi-disciplinary action in the face of socioecological complexity and limited data (Gibbs 2014; Adisasmito et al. 2022). Epidemiological models are powerful in understanding and responding to One Health challenges posed by zoonoses. Using the best-available science, epidemiological models can project the behavior of zoonotic disease spread across a range of possible conditions, quantify transmission risk between various host species, and examine the drivers influencing the introduction and transmission of zoonotic pathogens in wildlife hosts (Keeling and Rohani 2008). These exploratory inferences are particularly valuable with emerging infectious diseases and can complement monitoring efforts documenting the spatiotemporal distribution of infections (Plowright et al. 2019; Wilber et al. 2020).

Severe acute respiratory syndrome coronavirus 2 (SARS-CoV-2) in the subgenera *Sarbecoviruses*, subfamily *Orthocoronavirinae*, is a zoonotic virus that poses One Health challenges around the globe (Boni et al. 2020; Wu et al. 2020). SARS-CoV-2 infection can result in severe respiratory disease (known as COVID-19) and death in humans, yet in wildlife species SARS-CoV-2 severity is highly variable. Since it was first documented in humans in late 2019, the number of known SARS-CoV-2 hosts has increased and includes a range of companion and wild animals, including wild and captive white-tailed deer (*Odocoileus virginianus*; hereafter deer; Kuchipudi et al. 2022; EFSA panel 2023). Transmission of SARS-CoV-2 can occur

between humans, humans and animals, and between animals (Oude Munnink et al. 2021; Marques et al. 2022). Each of these transmission pathways is concerning from a public health perspective for several reasons. First, SARS-CoV-2 circulating in human and non-human hosts can persist, recombine, and evolve into novel variants that change the properties of this pathogen (Pickering et al. 2022; Tan et al. 2022; Yen et al. 2022; McBride et al. 2023. Second, non-human hosts can act as a reservoir for SARS-CoV-2, posing risks of SARS-CoV-2 persisting outside of human hosts (Gryseels et al. 2021; Caserta et al. 2023). Lastly, SARS-CoV-2 may spill back to humans from non-human hosts as a potentially more virulent form of SARS-CoV-2 (Oude Munnink et al. 2021). Collectively, these concerns have given rise to surveillance programs of SARS-CoV-2 in wild and captive white-tailed deer across North America (Bevins et al. 2023).

Two introduction pathways may have led to the transmission of SARS-CoV-2 from humans to deer, a process commonly referred to as 'spillover' (Figure 1). First, wild and captive deer could have been exposed to SARS-CoV-2 via direct interactions between humans and deer that are nearby. This direct pathway likely is a result of the aerosolized transmission of SARS-CoV-2 from humans to deer, given the tissue tropism in the upper respiratory tract of both species (Palmer et al. 2021; Martins et al. 2022). Direct interactions between humans and deer are possible in some areas of North America where deer are habituated to humans to the point where proximity or even contact is possible (Côté et al. 2004). Human-deer interactions are also common in captive settings, ranging from facilities and herd management activities to exposition opportunities for visitors. Second, deer could have been exposed to SARS-CoV-2 indirectly through contaminated surfaces, feed, water, or through intermediate animal hosts (Chandler et al.

2021). While this indirect pathway has been postulated, evidence of transmission through this pathway does not currently exist.

Like SARS-CoV-2 spillover from humans to deer, the spread of SARS-CoV-2 within a white-tailed deer population could also occur via direct and indirect pathways (Figure 1). Transmission between deer could occur given various social interactions in wild and captive settings, including various agonistic and mating behaviors (Hirth 1977; Schauber et al. 2015). Direct transmission of SARS-CoV-2 between deer might include aerosolized and fluid transmission. Aerosolized transmission of SARS-CoV-2 between deer could occur within captive facilities where deer densities are high or in wild settings when deer are near one another. Fluid exchange could also lead to the transmission amongst deer given social behaviors such as allogrooming in seasonal social groups (Marchinton and Hirth 1984). Indirect transmission of SARS-CoV-2 between deer may be possible through fomites, such as contaminated surfaces or feed, however, as previously mentioned, evidence of indirect transmission between deer is lacking.

Although our knowledge of SARS-CoV-2 has greatly increased over the last three years, factors influencing the introduction and transmission of SARS-CoV-2 in wildlife hosts and spillover risk remain poorly understood. Therefore, we develop a SIRS (Susceptible-Infected-Recovered-Susceptible) epidemiological model and apply it to wild and captive deer populations in a range of scenarios to address the following five objectives:

Objective 1: Evaluate human-deer (introduction) and deer-deer transmission (spread) in wild and captive deer scenarios to understand the role of pathways in disease dynamics;

Objective 2: Examine potential ranges of average prevalence, persistence, and incidence proportion of SARS-CoV-2 outbreaks in deer in wild and captive scenarios;

Objective 3: Understand the interaction among introduction, transmission, prevalence, persistence, and incidence proportion across all scenarios;

Objective 4: Test if SARS-CoV-2 outbreaks in deer require continual introduction from humans or just a single introduction event;

Objective 5: Identify how contact between deer in captive and wild scenarios through fence line interactions can influence SARS-CoV-2 prevalence and persistence system-wide.

Collectively, this study provides insights into the dynamics of SARS-CoV-2 outbreaks in white-tailed deer populations and provides evidence for different mechanisms of spillover and persistence. Our findings inform One Health efforts to reduce future introductions and transmission among white-tailed deer and diminish the risk of SARS-CoV-2 becoming enzootic in white-tailed deer across their North American range.

2. Methods

2.1. General approach and terms

We modeled SARS-CoV-2 transmission between humans and white-tailed deer, and among deer in several scenarios, including two types of captive facilities and wild deer in rural and suburban environments (Section 2.3). We estimated direct (aerosolized) transmission rates from humans to

143 deer as causing initial deer infections (human-to-deer, hereafter HtD; Section 2.3 & 2.4). We
144 estimated direct (aerosolized and fluid pathways) transmission rates within wild and captive deer
145 populations following introduction from humans (deer-to-deer, hereafter DtD; Section 2.3 &
146 2.4). We used these transmission rates to estimate two important epidemiological parameters
147 (Objective 1). The introduction of a pathogen, such as SARS-CoV-2 into deer populations, can
148 be quantified as the common Force-Of-Infection metric from humans to deer (FOI_{HD}; Figure 1;
149 Bjørnstad 2022). Then, SARS-CoV-2 transmission within a deer population can be quantified by
150 the basic reproductive metric, R_0, or the number of new infections, in a completely naive
151 population, originating from one infectious deer over the duration of its infection, with values
152 greater than one indicating sustained infection throughout a population and values less than one
153 indicating pathogen fade-out. (Figure 1; Bjørnstad 2022).
154
155 We projected the outbreak of infections across 120 days in each scenario to incorporate fall deer
156 behavior (September-December). We focused on the fall season as deer reproductive behavior
157 results in increased DtD contact rates and multiple hunting seasons and seasonal captive
158 activities could increase HtD interactions. We used these fall projections to estimate the
159 prevalence, persistence, and incidence proportion of SARS-CoV-2 in various types of simulated
160 white-tailed deer populations (Figure 1; Objective 2). We used our simulated data to investigate
161 the interaction between epidemiological parameters (introduction and transmission) and outbreak
162 characteristics in deer populations (prevalence, persistence, and incidence proportion; Objective
163 3). We contrasted outbreak dynamics from continuous introduction from humans, compared to
164 those from a single, initial infection event with no further introduction from humans (Objective
165 4). Finally, we ran the 120-day projection for wild and captive populations connected through a

166 single-layer fence to explore how interactions between captive and wild deer may influence the
167 prevalence and persistence of SARS-CoV-2 in both populations (Objective 5).
168
169 2.2. Epidemiological model
170
171 To understand SARS-CoV-2 transmission between humans and deer and within deer
172 populations, we developed a two-host (captive and wild deer) Susceptible-Infected-Recovered-
173 Susceptible (SIRS) model (Figure 2; Keeling and Rohani 2007). We considered two primary
174 introduction pathways, including aerosolized SARS-CoV-2 transmission in shared airspace, and
175 fluid transmission from sputum or other contagious discharges upon direct contact. For DtD
176 transmission, we integrated both transmission pathways, while for HtD transmission, we
177 estimated aerosolized transmission only. Humans were included as a source of infection, but
178 human disease dynamics were not modeled as a response to disease dynamics in deer.
179
180 We made several assumptions either inherent in our SIRS approach or that incorporate patterns
181 documented in the relevant literature. We assume that: transmission rates are additive;
182 transmission rates are the same for naïve susceptible deer and recovered deer that have lost
183 temporary immunity and are again susceptible; DtD transmission rates in wild scenarios and
184 captive scenarios mimic wild conditions and are intermediate between frequency- and density-
185 dependent transmission (see Section 2.2.1; Storm et al. 2013). DtD transmission rates in
186 intensive captive scenarios and across fence lines, and HtD transmission rates in all scenarios are
187 constant and frequency-dependent, based on available data (Section 2.3); DtD transmission rates
188 via fluids only occurs when an infected and a susceptible individual are in proximity, including

189 along fence lines; human prevalence is constant across each 120-day projection; there is
190 homogenous mixing within captive and wild deer populations; recovery from infection and loss
191 of immunity do not differ between captive and wild deer; there is no viral evolution; there is no
192 disease-induced mortality (Martins et al. 2022); there is no spillback from deer to humans (or at
193 least, such spillback does not affect the disease dynamics in the deer population); and deer
194 populations are closed, with no births, deaths, immigration, or emigration. On this last
195 assumption, we recognize that many deer are harvested in the season we chose to simulate. We
196 assume that harvest is random within the population such that the proportion of individuals
197 within the various disease compartments of the SIRS model are unaffected.
198
199 The SIRS model was specified with a system of six ordinary differential equations (ODE)
200 (Keeling and Rohani 2007; Section 2.2.1), and we derived rates for aerosolized and fluid
201 transmission (Sections 2.2.2 and 2.2.3, respectively). We tracked the fractions of a population
202 that are susceptible (s), infected (i), and recovered (r), rather than the number of individuals in
203 each compartment. Human prevalence is fixed and not explicitly modeled in this study (i_H). In
204 the equations that follow, our notation includes superscripts to indicate the mode of transmission,
205 including: “Aero”, to indicate transmission by aerosols; and “DC” to indicate transmission via
206 fluid exchanged through direct contact. We use subscripts to indicate the individuals in a
207 particular transmission interaction: transmission between wild deer (WW); transmission between
208 captive and wild deer (CW); transmission between captive deer (CC); transmission from humans
209 to wild deer (HW); and transmission from humans to captive deer (HC).
210
211 *2.2.1. Ordinary Differential Equation*

Three ODEs describe the disease dynamics in the wild deer population, with the daily change in the fraction of the wild population that is susceptible (s_W) given by

$$\frac{ds_W}{dt} = \alpha r_w - s_W(\beta_{WW}^{Aero} i_W + \beta_{WW}^{DC} i_W + \beta_{CW}^{Aero} i_C + \beta_{CW}^{DC} i_C + \beta_{HW}^{Aero} i_H), \quad (1)$$

the daily change in the fraction of the wild population that is infected (i_W) given by

$$\frac{di_W}{dt} = s_W(\beta_{WW}^{Aero} i_W + \beta_{WW}^{DC} i_W + \beta_{CW}^{Aero} i_C + \beta_{CW}^{DC} i_C + \beta_{HW}^{Aero} i_H) - \gamma i_W, \quad (2)$$

and the daily change in the fraction of the wild population that is recovered (r_W) given by

$$\frac{dr_W}{dt} = \gamma i_W - \alpha r_W, \quad (3)$$

where α is the immunity loss rate; β is the transmission rate specific to the infectious and susceptible host recipient type (e.g., wild or captive deer) and interactions (i.e., aerosolized or direct contact); and γ is the recovery rate from infection (Figure 2).

Three additional ODEs describe the disease dynamics in captive deer, with the daily change in the fraction of the captive population that is susceptible (s_C) given by

$$\frac{ds_C}{dt} = \alpha r_C - s_C(\beta_{CC}^{Aero} i_C + \beta_{CC}^{DC} i_C + \beta_{CW}^{Aero} i_W + \beta_{CW}^{DC} i_W + \beta_{HC}^{Aero} i_H), \quad (4)$$

the change in the fraction of the captive population that is infected (i_C) given by

$$\frac{di_C}{dt} = s_C(\beta_{CC}^{Aero} i_C + \beta_{CC}^{DC} i_C + \beta_{CW}^{Aero} i_W + \beta_{CW}^{DC} i_W + \beta_{HC}^{Aero} i_H) - \gamma i_C, \quad (5)$$

and the change in the fraction of the captive population that is recovered (r_C) given by

$$\frac{dr_C}{dt} = \gamma i_C - \alpha r_C. \quad (6)$$

We monitored proportions through these projections to reduce assumptions about population size in either wild or captive settings.

2.2.2. Aerosolized Transmission

Aerosolized transmission rates between a host *i* and recipient *j* (β_{ij}^{Aero}) can be described as

$$\beta_{ij}^{Aero} = \omega_{ij} * \sigma^{Aero} \quad (7)$$

where $\omega_{ij}$is the proximity rate between host-recipient(*i*,*j*) type (human-wild deer, human-captive deer, wild deer-wild deer, captive deer-captive deer, wild deer-captive deer, captive deer-wild deer); and σ^{Aero} is the probability of infection from aerosols.

We define proximity ω_{ij} as the frequency per day that host *i* and recipient *j* are within 1.5 meters (m) of each other, drawn from existing social distancing guidelines for humans which range from 1-2 meters (Chu et al. 2020; Feng et al. 2020). We estimate the proximity rate for wild deer, ω_{WW}, based on a contact rate model developed by Habib et al. (2011) for chronic wasting disease in white-tailed deer that permits density- or frequency-dependent transmission as well as intermediate cases that blend these two standard transmission processes. This rate applies to deer-deer transmission in most scenarios, including cases with and without attractants (e.g., bait, supplemental feed; see Section 2.3). We apply this model for captive circumstances that mimic natural conditions (see Section 2.3). It is given by

$$\omega_{ij} = \kappa\left(\frac{{N_W}^{(1-q)}}{A_W}\right) * \rho_{attractant} \quad (8)$$

where κ is a scaling constant; q is a concavity scaling constant of the density-contact rate relationship ranging from 0 – 1, which allows an intermediate blend of density-dependence to frequency-dependence, respectively (Habib et al. 2011); N_W is the total population size; A_W is the area inhabited by the population; $\rho_{attractant}$ is the adjustment for the presence of an attractant ($\rho_{attractant}$ = 1 indicates no attractants present; $\rho_{attractant}$ > 1 indicates attractants present).

All other proximity rates, including captive-captive deer (ω_{CC}), captive deer-wild deer (ω_{CW}), human-wild deer (ω_{HW}), and human-captive deer (ω_{HC}) were not explicitly modeled, and instead were drawn from parametric distributions (Section 2.3).

The probability of infection, σ^{Aero}, given proximity, is a function of the instantaneous dose received and a Wells-Riley dose-response relationship given by

$$\sigma^{Aero} = 1 - e^{-\theta Q} \quad (9)$$

where θ is the species-specific rate of infection from 1 quantum of SARS-CoV-2; and Q is the dose (quanta) received by a single contact with an infected individual. Buonanno et al. (2020) defines a quantum as "the dose of airborne droplet nuclei required to cause infections in 63% of susceptible human individuals." Therefore, $\theta > 1$ corresponds to 1 quantum causing infection in >63% of susceptible individuals, and $\theta < 1$ corresponds to 1 quantum causing infection in <63% of susceptible individuals (Wells 1934; Gammaitoni and Nucci 1997; Buonanno et al. 2020).

To estimate the dose received by a susceptible individual (Q) we modeled (1) the emission of SARS-CoV-2 from an infectious individual (ER_q) and (2) the resulting concentration of SARS-CoV-2 in a designated airspace around an infectious individual, considering viral emission and viral loss. First, an infected individual emits virions at a particular rate (ER_q; quanta/hr) as the product of the viral load in its exhalation (C_v; RNA copies/ml), a conversion factor (C_i; quanta/RNA copy), the inhalation/exhalation rate (IR; m^3/hr), and the exhaled droplet volume concentration (V_{drop}; ml droplets/m^3 exhaled; Mikszewski et al. 2021) given by

$$ER_q = C_v * C_i * IR * V_{drop}. \quad (10)$$

We then use the emission rate to model the instantaneous concentration of virions (C; quanta/m^3) in a well-mixed airspace (V_{air}; m^3) around an infected individual (ER_q; quanta/hr). We assumed that the airspace around an infected individual was a half-sphere with a radius of 1.5 m, or 7.07 m^3. We account for viral loss as the sum of air exchange (AER; hr^{-1}), settling (s; hr^{-1}), and inactivation (λ; hr^{-1}; modified from Buonanno et al. 2020). Thus, the instantaneous concentration is given by

$$C = \frac{ER_q}{(AER+s+\lambda)*V_{air}}. \quad (11)$$

When a susceptible individual enters the contaminated airspace surrounding an infectious individual, the dose (Q; quanta) is the product of the inhalation rate of the susceptible individual (IR; m^3/hr), the concentration of virions in the fixed volume (C; quanta/m^3), and the duration of contact ($t_{contact}$; hr) given by

$$Q = IR * C * t_{contact}. \quad (12)$$

2.2.3. Fluid transmission

We model fluid transmission rate for deer conditional on proximity with another deer (eqn. 8). Fluid transmission rates between a host and recipient (β_{ij}^{DC}) are given by

$$\beta_{ij}^{DC} = \omega_{ij} * \varepsilon^{DC} * \sigma^{DC} \quad (13)$$

where ω_{ij} is the proximity rate between host-recipient(ij) type (wild deer-wild deer, captive deer-captive deer, captive deer-wild deer); ε^{DC} is the probability of direct contact conditional on proximity; and σ^{DC} is the probability of infection from direct contact.

The probability of infection, σ^{DC}, given contact, was modeled similarly to eqn.9, as a log-logistic function of dose and the reciprocal probability of infection given exposure to a single dose, k (Watanabe et al. 2010). The dose received is a product of the transferred sputum volume given contact, V_{sputum}, and viral concentration in sputum, C_v given by

$$\sigma^{DC} = 1 - e^{-((C_v \times V_{sputum})/k)} \quad (14)$$

where C_v is the viral concentration in sputum (in plaque-forming units; PFU); V_{sputum} is the volume of sputum transferred given contact; and k is the reciprocal of the probability of a single PFU causing infection.

2.3. Scenario descriptions

We estimated HtD and DtD transmission and outbreak characteristics in four scenarios: (1) wild deer in a rural setting, (2) wild deer in a suburban setting, (3) captive deer in an outdoor ranch, and (4) captive deer in an intensive facility (Figure 2). These scenarios span a range of possible habitat or captive facility conditions, deer densities, and proximity rates with humans; although each of these variables is a continuous metric, we discretized the scenarios to make them easier to interpret.

346

347 Below, we present parameter estimates used in each simulation (Table 1). For parameters that
348 were unavailable in the literature, we conducted expert elicitation using the IDEA protocol and a
349 four-point elicitation process (Speirs-Bridge et al. 2010; Hanea et al. 2017). We included 11
350 experts on two separate panels: one focused on SARS-CoV-2 virology and another on deer
351 behavior in captive and wild settings. The estimates for 13 parameters we solicited from experts
352 are listed in Table 1. Experts and their affiliations, elicitation methods, the elicitation questions
353 for each panel, and individual (anonymous) and aggregated probability distributions are reported
354 in Supplemental Materials. For study Objectives 1 to 4, fence line transmission was fixed at zero
355 to capture outbreak dynamics within these specific scenarios. This transmission rate was restored
356 for the final study objective exploring the influence of linked scenarios across fence lines in
357 outbreak dynamics.

358

359 *Wild deer in a rural setting* – Wild deer are free-ranging in an area with a rural human density.
360 (3.1 humans/km^2; 15th percentile of U.S. counties with <100 humans/km^2 overlapping white-
361 tailed deer range; Pozzi and Small 2002; Walters et al. 2016; U.S. Census Bureau 2020, available
362 from: https://www.census.gov/geographies/mapping-files/time-series/geo/tiger-line-file.html).
363 We assumed that deer interacted with humans during regulated hunting either using still-hunting,
364 or ground blind or tree stand tactics but were not harvested. We also assumed that baiting and
365 backyard feeding were illegal but may still occur. We calculated wild DtD proximity rates using
366 a population density of 10 deer/km^2 for an area with 26% wooded habitat (Habib et al. 2011).
367 We assumed that Habib et al.'s (2011) estimated 25m proximity rate applied to our definition of
368 proximity of 1.5m for aerosol transmission. HtD transmission was derived by estimating the rate

and duration of human-deer proximity events and a fixed human prevalence of 5% (Table 1; Section 2.4). Wild deer in a rural setting had the lowest rate and duration of these human-deer proximity events (Table 1). We calculated and applied air-exchange rates (AER; 4^{-hr}) based on a 15-minute residence time drawn from a range of published values for forest airflow studies (Gerken et al. 2017; Bannister et al. 2023; Table 1).

Wild deer in a suburban setting – Wild deer are free-ranging in an area of suburban human density (100 humans/km^2; Pozzi and Small 2002). DtD proximity rates were derived using the same parameters as used in the rural scenario, and the AER value used was the same as in the rural scenario (Table 1). Wild deer in a suburban setting experience higher HtD transmission rates, driven by higher HtD proximity rates and longer duration of proximity events, relative to wild deer in a rural setting (Section 2.4; Table 1).

Captive deer in an outdoor ranch – We considered captive deer in an outdoor ranch facility typical of a managed, fenced hunting reserve. We assumed that deer stocking densities resulted in the same DtD proximity rates as were estimated in wild scenarios, with an increase in proximity rates due to supplemental feeding (Section 2.4; Table 1). We used the same AER value as in wild settings as these captive individuals reside outside. We assume HtD proximity rates are the same as those estimated for the "wild deer in a suburban setting" scenario, but the typical duration of these proximity events is longer in this scenario, reflecting those typical of a captive facility (Table 1).

391 *Captive deer in an intensive facility* – The last scenario considered was captive deer in a captive
392 breeding or exposition facility. Deer in this type of facility were predominantly indoors at high
393 stocking densities and low indoor air exchange rates (AER; 1^{-hr}). Both DtD and HtD proximity
394 rates and duration were highest in this scenario (Section 2.4; Table 1).
395
396 *Objective 1: Differences in human-to-deer and deer-to-deer transmission across scenarios* – We
397 quantified the strength of HtD transmission in each scenario using Force-of-Infection
398 calculations from humans to deer (FOI_{HD}; eqn. 15). These FOI calculations are based on HtD
399 transmission rates (β_{HD}^{Aero}; eqn. 7) and human prevalence (i_H) and equate to the proportion of
400 susceptible deer infected by infectious humans per day.
401
402 $$FOI_{HD} = \beta_{HD}^{Aero} i_H \quad (15)$$
403
404 We also report the probability of at least one HtD transmission per 1,000 deer (N) over the fall
405 season (t = 120 days), using a constant hazard model (Kalbfleisch and Prentice 2011; eqn 16).
406
407 $$p(HtD|FOI_{HD}, N, t) = 1 - (e^{-FOI_{HD}t})^N \quad (16)$$
408
409 We quantified the strength of DtD transmission for each scenario using the number of
410 susceptible deer infected by a single infectious deer, R_0, derived from the sum of aerosol and
411 fluid transmission rates over the recovery period from infection (γ; eqn. 17). Again, R_0 values
412 greater than one indicate sustained transmission throughout a population, and values less than
413 one indicate pathogen fade-out.

$$R_0 = \frac{\beta_{ij}^{Aero} + \beta_{ij}^{DC}}{\gamma}. \quad (17)$$

We compare FOI_{HD}, *p(HtD)*, and R_0 estimates across scenarios to evaluate differences in the potential for SARS-CoV-2 to be transmitted from humans to deer and then spread amongst deer. All calculations were conducted in R (R Core Team 2023).

Objective 2: Average prevalence, persistence of infection, and incidence proportion in each scenario – We used the six ODEs for the SIRS model, parameters estimated from the literature or expert elicitation, and derived transmission parameters to project continual SARS-CoV-2 introduction and spread across each scenario of interest (Table 1). From these projections, we calculated the proportion of individuals in the wild, captivity, or in both settings that were susceptible, infectious, or recovered. We ran 1,000 iterations for each of the four scenarios. Each iteration had a randomly drawn parameter set, where we randomly drew one value from each parameter distribution during each iteration, resulting in 1,000 parameter sets used to project outbreaks in each scenario (Table 1). Parameters that were constant across scenarios did not vary between parameter sets which ensured that any observed variation was due to differences across scenarios, and not sampling variation from repeated random draws from error distributions.

We projected the proportional size of each SIRS compartment for 120 days for each iteration, using the ODE solver *ode()* from the deSolve package in R (Soetaert et al. 2010; R Core Team 2023). We estimated the average daily prevalence of deer in each scenario during the 120-day projection. We determined if SARS-CoV-2 would persist beyond the 120-day projection for each

iteration using the *runsteady()* function from the rootSolve package (Soetaert 2009; Soetaert and Herman 2009) to estimate the deterministic stable state from the SIRS ODE equation. We assigned each iteration a logical value if infectious compartment at equilibrium was >0.1% for each iteration (at least 1 deer infected out of 1 000). We estimated mean probability of persistence and 95% binomial confidence intervals using the *binom.confint()* function with the exact method from the binom package for each scenario (Dorai-Raj 2022). Finally, we tracked the incidence proportion, or cumulative proportion of the population infected over the 120 days during these simulations for wild and captive deer (eqn. 18 and 19). This incidence proportion could exceed 1, indicating that all individuals in the population were infected at least once.

$$Incidence\ proportion_W = \sum_{t=1}^{120} s_{W,t-1}\left(\beta_{WW}^{Aero} i_{W,t-1} + \beta_{WW}^{DC} i_{W,t-1} + \beta_{CW}^{Aero} i_{C,t-1} + \beta_{CW}^{DC} i_{C,t-1} + \beta_{HW}^{Aero} i_H\right) \quad (18)$$

$$Incidence\ proportion_C = \sum_{t=1}^{120} s_{C,t-1}\left(\beta_{CC}^{Aero} i_{C,t-1} + \beta_{CC}^{DC} i_{C,t-1} + \beta_{CW}^{Aero} i_{W,t-1} + \beta_{CW}^{DC} i_{W,t-1} + \beta_{HC}^{Aero} i_H\right) \quad (19)$$

We summarized these three measures across iterations in each scenario with the median value and 80% confidence intervals. These include median average prevalence, median probability of persistence, and median incidence proportion.

458 *Objective 3: Interaction between spillover, spread, prevalence, and persistence* – After each
459 iteration, we categorized outcomes by one of the following spread categories: unsustained spread
460 (R_0 <1), low, sustained spread (1< $R_0 \leq 3$), medium, sustained spread (3 < $R_0 \leq 5$), and high,
461 sustained spread ($R_0 > 5$). We used the *stat-smooth()* function from the ggplot2 package (Hadley
462 2016) to visualize trends between HtD transmission, as quantified by FOI, prevalence, and
463 persistence of SARS-CoV-2 for each spread category.
464
465 *Objective 4: SARS-CoV-2 outbreaks in deer from a single introduction event* – We tested
466 whether a SARS-CoV-2 outbreak can occur following a single spillover event, in contrast to the
467 continual introduction modeled above for the other objectives. We simulated this introduction as
468 an initial event that resulted in 0.1%, 1e-4 %, and 1e-7 % prevalence in deer at the start of the
469 120-day projection, with no further introduction from humans. We compared differences in
470 prevalence, incidence proportion, and persistence between these initial spillover simulations and
471 the continuous spillover simulation investigated for the other objectives.
472
473 *Objective 5 Effects of fence line interactions between wild and captive deer on SARS-CoV-2*
474 *prevalence and persistence on either side of the fence* – We extended our SIRS model to allow
475 fence line interactions between captive and wild deer. To do this we projected outbreaks for
476 paired captive -wild scenarios separated by a fence, using combinations of the two captive and
477 two wild scenarios and associated parameters described above (n = 4 combinations; hereafter
478 systems). We added fence line contact probability and allowed all individuals to interact along
479 fence lines, enabling proximity and direct contact (Table 1).
480

3. Results

3.1. Objective 1: Differences of introduction and spread for white-tailed deer across settings

The risk of introduction of SARS-CoV-2 from humans to deer varied within and across scenarios (eqn 15 and 16, respectively; Figure 3; Table 2). Median FOI_{HD} estimates were 219-, 85-, and 19-times higher in the intensive facility, outdoor ranch, and wild deer in suburban scenarios, respectively, relative to median FOI_{HD} estimates for rural, wild deer (Table 2). Median probabilities of at least one HTD transmission per 1000 deer ranged from 88%, 56.1%, 17.7%, and 1.1% in the intensive facility, outdoor ranch, wild suburban, and wild rural scenarios, respectively (Table 2). There was high uncertainty around risk of introduction in each scenario, with detectable differences between the intensive facility and wild deer in rural setting using 80% confidence intervals (Table 2). SARS-CoV-2 transmission between deer (R_0; eqn 18) was greater in captive scenarios relative to wild scenarios, with most iterations sustaining transmission of SARS-CoV-2 among the deer population (Table 2). Transmission in both wild scenarios were nearly identical, with most iterations resulting in R_0 values too small to sustain transmission of SARS-CoV-2 (median R_0 = 0.97; Table 2). R0 values were highly variable in each scenario leading to no detectable differences with 80% confidence (Table 2).

3.2. *Objective 2: Average prevalence, persistence of infection, and incidence proportion in each setting*

Simulated outbreaks of SARS-CoV-2 were variable across scenarios, with higher average prevalence, incidence proportions, and probability of persistence in captive scenarios relative to wild scenarios (Table 2; Figure 4). Intensive facilities had the highest average prevalence,

incidence proportion, and probability of SARS-CoV-2 persistence, followed by the outdoor ranch scenario and both wild scenarios (Table 2). Median outbreak metrics in both wild scenarios, while much lower than captive scenarios, were slightly elevated in the suburban setting compared to the rural setting (Table 2). Overall, there was high variability in these metrics in each scenario, with non-overlapping 80% confidence for the probability of persistence in the intensive facility, outdoor ranch, and wild scenarios (Table 2; Figure 4).

3.3. Objective 3: Interaction between spillover, transmission, prevalence, incidence proportion, and persistence

When we partitioned the relationship between FOI_{HD} and outbreak characteristics, we found compelling evidence that FOI_{HD} differs depending on how quickly SARS-CoV-2 transmits (R_0, Figure 5). When transmission is too low to sustain SARS-CoV-2 (R_0 <1 deer infected by an infected deer), high FOI_{HD} is required for non-zero average prevalence and incidence proportion during the projection, and for a high probability of infections persisting past the 120-day projection (Figure 5). As transmission reaches self-sustaining levels (1< R_0 <3 deer infected by an infected deer), the role of FOI_{HD} has a greater influence on average prevalence, incidence proportion, and persistence (Figure 5). As R_0 continues to increase to medium (3< $R_0 \leq 5$ deer infected by an infected deer) and high spread (R_0 > 5 deer infected by an infected deer), the influence of FOI_{HD} on prevalence and incidence proportion diminishes, and persistence is no longer sensitive to changes in FOI_{HD}. (Figure 5).

3.4. Objective 4: SARS-CoV-2 outbreaks in deer from a single introduction event

Differences in outbreak characteristics exist between continual introduction of SARS-CoV-2 from humans and a single, initial introduction (Figure 6). However, these differences vary depending on the size of the initial introduction and the scenario and uncertainty prevented high confidence in these differences. If an initial, single introduction resulted in 0.1% prevalence in any context, the average prevalence and incidence proportion were slightly greater than the average prevalence and incidence proportion when SARS-CoV-2 was continuously introduced. However, probability of persistence decreased in all scenarios except for wild deer in a rural setting, where probability of persistence would increase with this initial prevalence compared to when SARS-CoV-2 was continuously introduced. With an initial prevalence of 0.0001%, all scenarios showed median average prevalence and incidence proportion similar to or slightly lower than when SARS-CoV-2 was continuously introduced. The probability of persistence was consistent with those estimated for an initial 0.1% prevalence. Finally, with an initial prevalence of 1e-7%, the lowest tested, all scenarios showed decreases in average prevalence, probability of persistence, and incidence proportion relative to other continuous or initial infection conditions. However, even at this low level of initial infection, deer in the intensive facility scenario had median average prevalence and median incidence proportion that were comparable to when SARS-CoV-2 was continuously introduced, albeit with greater variability.

3.5. *Objective 5: Effects of fence line interactions between wild and captive deer on SARS-CoV-2 prevalence and persistence on either side of the fence*

When fence line interactions occurred between all combinations of captive and wild scenarios, wild deer had a higher prevalence and incidence proportion of SARS-CoV-2 during the fall projection compared to simulations without fence line interactions (Objective 2; Table 3). These

549 increases were highly variable depending on the captive and wild conditions. The probability for
550 persistence did not increase for wild deer when fence line interactions occurred, and captive deer
551 did not experience an increase in any metric (Table 3). Of the four systems, fence line
552 interactions had the greatest effect when dividing captive deer in an intensive facility and wild
553 deer in a rural setting. In this system during the 120-day projection, the average prevalence in
554 wild deer increased by approximately 122% (median), and the incidence proportion of the wild
555 deer in a rural setting increased from 1e-5 to 0.278 (median, Table 3). Smaller increases were
556 estimated in the intensive facility and wild deer in a suburban system (Table 3). We estimated
557 similar patterns when considering systems with fence line interactions between outdoor ranch
558 facilities and wild deer, albeit smaller in magnitude (Table 3).
559
560 4. Discussion
561
562 Our study demonstrates the potential for variable, yet widespread risk of SARS-COV-2
563 introduction and spread across white-tailed deer populations in North America. Our findings
564 indicated that the sociality of white-tailed deer and various environmental contexts may lead to
565 sustained transmission. We estimated sustained infections in wild and captive populations across
566 a wide range of infection risks from both continuous transmission from humans and an initial
567 transmission event. We also demonstrated that wild deer may experience higher prevalence,
568 incidence proportion, and persistence of SARS-CoV-2 infections when sharing a fence line with
569 captive facilities. These results complement ongoing, retrospective surveillance efforts across a
570 range of captive and wild contexts by revealing the spillover risk of SARS-CoV-2 from infected
571 humans and the risk of transmission between deer. More broadly, our approach provides a

framework for using epidemiological modeling to evaluate the risks of outbreaks and sustained infections of SARS-CoV-2 and other zoonotic diseases in wildlife hosts in a variety of contexts.

Despite lower risks of introduction and transmission, SARS-CoV-2 was still able to transmit and sustain itself in wild scenarios. If R_0 was less than one, indicating unsustainable transmission, our two wild scenarios did not have sufficient FOI_{HD} to sustain infections. However, when R_0 increased above one, wild scenarios showed rapid increases in average prevalence and incidence proportion, and a high probability of SARS-CoV-2 persisting into the future. Our findings generally match those reported by Hewitt et al. (2023), who used surveillance data from wild deer across the United States of America to estimate infection rates and prevalence, and estimated R_0 greater than 1 in most of counties monitored across 27 states. In short, our results indicate that there may be broad circumstances where wild deer populations could face repeated introduction and sustained transmission of SARS-CoV-2.

Both captive scenarios showed a higher risk of introduction and a higher rate of transmission, resulting in higher prevalence and persistence relative to wild scenarios. Our findings conform to the available literature on the introduction and transmission of SARS-CoV-2 in captive populations. Roundy et al. (2022) reported 94.4% seropositivity for one captive herd and 0% seropositivity in two other captive herds, one of which housed axis (*Axis axis*) and fallow deer (*Dama dama*). This contrast could indicate a difference in transmission from humans, as stocking conditions may increase the transmission of the virus. Our study also indicated different epidemiological dynamics in systems where captive and wild deer may interact through fence lines compared to systems without these interactions. However, despite the vulnerabilities of

595 captive conditions to rapid transmission of SARS-CoV-2, we emphasize that the patterns of
596 outbreaks in facilities and increased risk of fence line transmission are likely to vary through
597 space and time. Our captive scenarios did not focus on single facilities with a particular herd
598 size, but rather a pool of captive individuals. Introduction and transmission within individual
599 facilities may be so rapid that a localized infection results in SARS-CoV-2 running out of
600 susceptible hosts and the outbreak extinguishing itself. Spillover to wild populations through
601 fence line interactions during localized outbreaks remain a risk for these individual facilities,
602 though the risk of spillover from wild to captive facilities appears low.
603
604 White-tailed deer encounter a wide range of conditions across North America making it
605 challenging to capture this variability in a single analysis. The four scenarios evaluated here are
606 indicative of processes typical of both wild and captive conditions. Our analysis focused on
607 temporal patterns of SARS-CoV-2 introduction and spread across wild and captive white-tailed
608 deer, yet spatial variation undoubtedly plays a role. We did not make our simulations spatially
609 explicit, as we felt that our global approach met our objectives to better understand infection
610 dynamics across typical conditions. Additionally, integrating a spatial component to this study
611 would require specific spatial conditions and assumptions that either generalize across large
612 geographic extents, or limit inferences to conditions in a specific locality. We feel these are
613 important next steps given our inferences from this study and will aid in our understanding of the
614 reported spatial and temporal heterogeneities of SARS-CoV-2 cases in white-tailed deer
615 (Chandler et al. 2021; Kuchipudi et al. 2022; Willgert et al. 2022; Caserta et al. 2023).
616

We were required to make several assumptions in our parameterization of the SIRS models that may have influenced our inferences. First, we used Watanabe et al.'s (2010) reported infection probability for SARS-CoV in mice by intranasal exposure to estimate transmission of SARS-CoV-2 through fluid when deer make physical contact. We join other simulation studies that use this parameter estimate to calculate direct contact probability through fluid transfer and acknowledge the uncertainty of this parameter given it has not been quantified in the literature (Pitol and Julian 2021). Second, we used the stable-state equilibrium of the SIRS model to infer the persistence of SARS-CoV-2. We acknowledge that this assumes that parameter values are not stochastic and do not change past the simulated fall season. Seasonal changes in white-tailed deer behavior are well-documented and affect introduction and spread for multiple pathogens in deer, as with other host-pathogen systems (Altizer et al. 2006; Grassly and Fraser 2006; Williams et al. 2014). Third, parameters used to derive transmission risk between deer in our simulations did not vary by sex. Ongoing monitoring of SARS-CoV-2 in wild white-tailed deer populations indicate higher infection probability and seropositivity in male white-tailed deer, likely driven by sex-specific behaviors (Hale et al. 2022; Hewitt et al. 2023). We believe that our inferences are robust with our integration of uncertainty around derived parameter estimates and the patterns of prevalence and persistence values documented in multiple studies monitoring ongoing infections (McBride et al. 2023).

Despite a growing number of studies of SARS-CoV-2 in white-tailed deer, there is no consensus on how SARS-CoV-2 is introduced into deer populations. This is a key detail in mitigating the introduction and transmission of SARS-CoV-2 in a prolific wildlife species that can interact with humans in both wild and captive contexts. In this study, an initial outbreak had to infect less than

10e-7% of deer for there to be an observable decrease in average prevalence, incidence proportion, and probability of persistence compared to those observed during continual spillover. These results indicate that an initial introductory event, even at a low rate, could result in an outbreak in both captive and wild settings. While introduction through aerosolized transmission from humans to deer is presumed to be most probable, our findings indicate that indirect sources of infection could play a role through a single transmission event. Infection from contaminated fomites or wastewater could initiate an outbreak given sufficient dose received by an individual. However, further research remains into the risk posed by these sources.

Sustained SARS-CoV-2 infections in this prolific wildlife species frequently interacting with humans in captive and wild settings creates a One Health challenge that affects human, animal, and ecosystem health. SARS-CoV-2 has demonstrated its ability to spread in wild and captive white-tailed deer populations across much of North America. The outbreak dynamics reported in this study indicate the ease by which the virus can be introduced and sustained in this non-human species. Surveillance studies indicate that multiple lineages of SARS-CoV-2 have been introduced and broadly circulated in white-tailed deer populations (Kuchipudi et al. 2022; Marques et al. 2022; Caserta et al. 2023), with evidence of spillback from deer to humans (Pickering et al. 2022; Feng et al. 2023). Our modeling approach provides a foundation to evaluate risks to human, animal, and ecosystem health posed by zoonotic diseases, and to test potential interventions to meet this and other One Health challenges.

5. Acknowledgments

We thank Paul Cross, Anna Fagre, Kate Huyvaert, Jeff Root, Jeff Chandler, Sarah Hamer, Kamen Campbell, Chris Jennelle, Jonathan Trudeau, Kurt Vandegrift, and Noelle Thompson for their participation in our expert elicitations. Any use of trade, firm, or product names is for descriptive purposes only and does not imply endorsement by the U.S. Government. This is publication #05 of the Disease Decision Analysis and Research Group (DDAR) of the U.S. Geological Survey.

6. Data availability statement

All code and generated data used in this study are available in the R software package whitetailedSIRS (Rosenblatt et al. 2023).

7. Funding

This work was supported by the Coronavirus Aid, Relief, and Economic Security Act (P.L. 116-136). This research was supported in part by the U.S. Department of Agriculture, Animal and Plant Health Inspection Service.

8. Literature Cited

Adisasmito, W.B., Almuhairi, S., Behravesh, C.B., Bilivogui, P., Bukachi, S.A., Casas, N., Becerra, N.C., Charron, D.F., Chaudhary, A., Zanella, J.R.C. and Cunningham, A.A.,

685 2022. One Health: A new definition for a sustainable and healthy future. PLoS
686 Pathogens, 18(6), p.e1010537.
687
688 Altizer, S., Dobson, A., Hosseini, P., Hudson, P., Pascual, M. and Rohani, P., 2006. Seasonality
689 and the dynamics of infectious diseases. Ecology letters, 9(4), pp.467-484.
690
691 Bannister, E.J., Jesson, M., Harper, N.J., Hart, K.M., Curioni, G., Cai, X., and MacKenzie, A.R.,
692 2023. Residence times of air in a mature forest: observational evidence from a free-air
693 CO 2 enrichment experiment. Atmospheric Chemistry and Physics, 23(3), pp.2145-2165.
694
695 Bevins, S., Chipman, R.B., Beckerman, S.F., Bergman, D.L., Collins, D.T., Deliberto, T.J.,
696 Eckery, J.P., Ellis, J.W., Gosser, A.L., Heale, J.D. and Klemm, J.M., 2023. SARS-CoV-2
697 occurrence in white-tailed deer throughout their range in the conterminous United States.
698 bioRxiv, pp.2023-04.
699
700 Boni, M.F., Lemey, P., Jiang, X., Lam, T.T.Y., Perry, B.W., Castoe, T.A., Rambaut, A. and
701 Robertson, D.L., 2020. Evolutionary origins of the SARS-CoV-2 sarbecovirus lineage
702 responsible for the COVID-19 pandemic. Nature Microbiology, 5(11), pp.1408-1417.
703
704 Bjørnstad, O.N., 2022. Epidemics: models and data using R. Springer Nature.
705

706 Buonanno, G., Stabile, L. and Morawska, L., 2020. Estimation of airborne viral emission:
707 Quanta emission rate of SARS-CoV-2 for infection risk assessment. Environment
708 International, 141, p.105794.
709
710 Caserta, L.C., Martins, M., Butt, S.L., Hollingshead, N.A., Covaleda, L.M., Ahmed, S., Everts,
711 M.R., Schuler, K.L. and Diel, D.G., 2023. White-tailed deer (Odocoileus virginianus)
712 may serve as a wildlife reservoir for nearly extinct SARS-CoV-2 variants of concern.
713 Proceedings of the National Academy of Sciences, 120(6), p.e2215067120.
714
715 Chandler, J.C., Bevins, S.N., Ellis, J.W., Linder, T.J., Tell, R.M., Jenkins-Moore, M., Root, J.J.,
716 Lenoch, J.B., Robbe-Austerman, S., DeLiberto, T.J. and Gidlewski, T., 2021. SARS-
717 CoV-2 exposure in wild white-tailed deer (Odocoileus virginianus). Proceedings of the
718 National Academy of Sciences, 118(47), p.e2114828118.
719
720
721 Chu, D.K., Akl, E.A., Duda, S., Solo, K., Yaacoub, S., Schünemann, H.J., El-Harakeh, A.,
722 Bognanni, A., Lotfi, T., Loeb, M. and Hajizadeh, A., 2020. Physical distancing, face
723 masks, and eye protection to prevent person-to-person transmission of SARS-CoV-2 and
724 COVID-19: a systematic review and meta-analysis. The Lancet, 395(10242), pp.1973-
725 1987.
726
727 Côté, S.D., Rooney, T.P., Tremblay, J.P., Dussault, C. and Waller, D.M., 2004. Ecological
728 impacts of deer overabundance. Annu. Rev. Ecol. Evol. Syst., 35, pp.113-147.

Dorai-Raj, S. 2022. binom: Binomial Confidence Intervals for Several Parameterizations. R package version 1.1-1.1, <https://CRAN.R-project.org/package=binom>.

EFSA Panel on Animal Health and Welfare (AHAW), Nielsen, S.S., Alvarez, J., Bicout, D.J., Calistri, P., Canali, E., Drewe, J.A., Garin-Bastuji, B., Gonzales Rojas, J.L., Gortázar, C. and Herskin, M., 2023. SARS-CoV-2 in animals: susceptibility of animal species, risk for animal and public health, monitoring, prevention and control. EFSA Journal, 21(2), p.e07822.

Feng, A., Bevins, S., Chandler, J., DeLiberto, T.J., Ghai, R., Lantz, K., Lenoch, J., Retchless, A., Shriner, S., Tang, C.Y. and Tong, S.S., 2023. Transmission of SARS-CoV-2 in free-ranging white-tailed deer in the United States. Nature Communications, 14(1), p.4078.

Feng, Y., Marchal, T., Sperry, T. and Yi, H., 2020. Influence of wind and relative humidity on the social distancing effectiveness to prevent COVID-19 airborne transmission: A numerical study. Journal of aerosol science, 147, p.105585.

Gammaitoni, L. and Nucci, M.C., 1997. Using a mathematical model to evaluate the efficacy of TB control measures. Emerging infectious diseases, 3(3), p.335.

Gerken, T., Chamecki, M., and Fuentes, J.D., 2017. Air-parcel residence times within forest canopies. Boundary-Layer Meteorology, 165, pp.29-54.

Gibbs, E.P.J., 2014. The evolution of One Health: a decade of progress and challenges for the future. Veterinary Record, 174(4), pp.85-91.

Grassly, N.C. and Fraser, C., 2006. Seasonal infectious disease epidemiology. Proceedings of the Royal Society B: Biological Sciences, 273(1600), pp.2541-2550.

Gryseels, S., De Bruyn, L., Gyselings, R., Calvignac-Spencer, S., Leendertz, F.H. and Leirs, H., 2021. Risk of human-to-wildlife transmission of SARS-CoV-2. Mammal Review, 51(2), pp.272-292.

Habib, T.J., Merrill, E.H., Pybus, M.J. and Coltman, D.W., 2011. Modelling landscape effects on density–contact rate relationships of deer in eastern Alberta: implications for chronic wasting disease. Ecological Modelling, 222(15), pp.2722-2732.

Hale, V.L., Dennis, P.M., McBride, D.S., Nolting, J.M., Madden, C., Huey, D., Ehrlich, M., Grieser, J., Winston, J., Lombardi, D. and Gibson, S., 2022. SARS-CoV-2 infection in free-ranging white-tailed deer. Nature, 602(7897), pp.481-486.

Hanea, A.M., McBride, M.F., Burgman, M.A., Wintle, B.C., Fidler, F., Flander, L., Twardy, C.R., Manning, B. and Mascaro, S., 2017. Investigate Discuss Estimate Aggregate for structured expert judgement. International journal of forecasting, 33(1), pp.267-279.

775 Hewitt, J., Wilson-Henjum, G., Collins, D., Linder, T., Lenoch, J., Heale, J., Quintanal, C.,
776 Pleszewski, R., McBride, D., Bowman, A. and Chandler, J., 2023. Epidemiological
777 dynamics of SARS-CoV-2 in white-tailed deer.
778
779 Hirth, D.H., 1977. Social behavior of white-tailed deer in relation to habitat. Wildlife
780 Monographs, (53), pp.3-55.
781
782 Kalbfleisch, J.D. and Prentice, R.L., 2011. The statistical analysis of failure time data. John
783 Wiley & Sons.
784
785 Keeling, M.J., and Rohani, P., 2008. Modeling Infectious Diseases in Humans and Animals.
786 Princeton University Press, Princeton, New Jersey
787
788 Kuchipudi, S.V., Surendran-Nair, M., Ruden, R.M., Yon, M., Nissly, R.H., Vandegrift, K.J.,
789 Nelli, R.K., Li, L., Jayarao, B.M., Maranas, C.D. and Levine, N., 2022. Multiple
790 spillovers from humans and onward transmission of SARS-CoV-2 in white-tailed deer.
791 Proceedings of the National Academy of Sciences, 119(6), p.e2121644119.
792
793 Marchinton R. L. and Hirth D. H., 1984. Behavior. Pp. 129–168 in Ecology and management of
794 white-tailed deer (Halls L. K., ed.). Stackpole Publishing Co., Harrisburg, Pennsylvania.
795
796 Marques, A.D., Sherrill-Mix, S., Everett, J.K., Adhikari, H., Reddy, S., Ellis, J.C., Zeliff, H.,
797 Greening, S.S., Cannuscio, C.C., Strelau, K.M. and Collman, R.G., 2022. Multiple

introductions of SARS-CoV-2 Alpha and Delta variants into white-tailed deer in Pennsylvania. MBio, 13(5), pp.e02101-22.

Martins, M., Boggiatto, P.M., Buckley, A., Cassmann, E.D., Falkenberg, S., Caserta, L.C., Fernandes, M.H., Kanipe, C., Lager, K., Palmer, M.V. and Diel, D.G., 2022. From Deer-to-Deer: SARS-CoV-2 is efficiently transmitted and presents broad tissue tropism and replication sites in white-tailed deer. PLoS Pathogens, 18(3), p.e1010197.

McBride, D., Garushyants, S., Franks, J., Magee, A., Overend, S., Huey, D., Williams, A., Faith, S., Kandeil, A., Trifkovic, S. and Miller, L., 2023. Accelerated evolution of SARS-CoV-2 in free-ranging white-tailed deer.

Oude Munnink, B.B., Sikkema, R.S., Nieuwenhuijse, D.F., Molenaar, R.J., Munger, E., Molenkamp, R., Van Der Spek, A., Tolsma, P., Rietveld, A., Brouwer, M. and Bouwmeester-Vincken, N., 2021. Transmission of SARS-CoV-2 on mink farms between humans and mink and back to humans. Science, 371(6525), pp.172-177.

Palmer, M.V., Martins, M., Falkenberg, S., Buckley, A., Caserta, L.C., Mitchell, P.K., Cassmann, E.D., Rollins, A., Zylich, N.C., Renshaw, R.W. and Guarino, C., 2021. Susceptibility of white-tailed deer (Odocoileus virginianus) to SARS-CoV-2. Journal of virology, 95(11), pp.e00083-21.

821 Pickering, B., Lung, O., Maguire, F., Kruczkiewicz, P., Kotwa, J.D., Buchanan, T., Gagnier, M.,
822 Guthrie, J.L., Jardine, C.M., Marchand-Austin, A. and Massé, A., 2022. Divergent
823 SARS-CoV-2 variant emerges in white-tailed deer with deer-to-human transmission.
824 Nature Microbiology, pp.1-14.
825
826 Plowright, R.K., Becker, D.J., McCallum, H. and Manlove, K.R., 2019. Sampling to elucidate
827 the dynamics of infections in reservoir hosts. Philosophical Transactions of the Royal
828 Society B, 374(1782), p.20180336.
829
830 Pitol, A.K. and Julian, T.R., 2021. Community transmission of SARS-CoV-2 by surfaces: risks
831 and risk reduction strategies. Environmental Science & Technology Letters, *8*(3), pp.263-
832 269.
833
834 Pozzi, F. and Small, C., 2002. Vegetation and population density in urban and suburban areas in
835 the USA. In Third International Symposium of Remote Sensing of Urban Areas (pp. 1-6).
836
837 R Core Team 2023. R: A language and environment for statistical computing. R Foundation for
838 Statistical Computing, Vienna, Austria. https://www.R-project.org/.
839
840 Rahman, M.T., Sobur, M.A., Islam, M.S., Ievy, S., Hossain, M.J., El Zowalaty, M.E., Rahman,
841 A.T. and Ashour, H.M., 2020. Zoonotic diseases: etiology, impact, and control.
842 Microorganisms, 8(9), p.1405.
843

844 Roundy, C.M., Nunez, C.M., Thomas, L.F., Auckland, L.D., Tang, W., Richison III, J.J., Green,
845 B.R., Hilton, C.D., Cherry, M.J., Pauvolid-Corrêa, A. and Hamer, G.L., 2022. High
846 seroprevalence of SARS-CoV-2 in white-tailed deer (Odocoileus virginianus) at one of
847 three captive cervid facilities in Texas. Microbiology Spectrum, 10(2), pp.e00576-22.
848
849 Rosenblatt, E, Rudolph, J.F., Arce, F., Cook, J. D., DiRenzo, G.V., Grant, E.H.C., Runge, M.C.,
850 and Mosher, B.A., 2023. whitetailedSIRS: A package to project SARS-CoV-2 outbreak
851 dynamics in white-tailed deer. Version 1.0.0: U.S. Geological Survey software release,
852 https://doi.org/10.5066/P9TZK938
853
854 Schauber, E.M., Nielsen, C.K., Kjær, L.J., Anderson, C.W. and Storm, D.J., 2015. Social
855 affiliation and contact patterns among white-tailed deer in disparate landscapes:
856 implications for disease transmission. Journal of Mammalogy, 96(1), pp.16-28.
857
858 Soetaert, K., 2009. rootSolve: Nonlinear root finding, equilibrium and steady-state analysis of
859 ordinary differential equations. R-package version 1.6.
860
861 Soetaert, K. and Herman, P.M.J., 2009. A Practical Guide to Ecological Modelling. Using R as a
862 Simulation Platform. Springer, 372 pp.
863
864 Soetaert, K., Petzoldt, T. and Setzer, R.W., 2010. Solving differential equations in R: Package
865 deSolve. Journal of Statistical Software, 33(9), 1--25. doi:10.18637/jss.v033.i09
866

867 Speirs-Bridge, A., Fidler, F., McBride, M., Flander, L., Cumming, G. and Burgman, M., 2010.
868 Reducing overconfidence in the interval judgments of experts. Risk Analysis: An
869 International Journal, 30(3), pp.512-523.
870
871 Storm, D.J., Samuel, M.D., Rolley, R.E., Shelton, P., Keuler, N.S., Richards, B.J. and Van
872 Deelen, T.R., 2013. Deer density and disease prevalence influence transmission of
873 chronic wasting disease in white-tailed deer. Ecosphere, 4(1), pp.1-14.
874
875 Tan, C.C., Lam, S.D., Richard, D., Owen, C.J., Berchtold, D., Orengo, C., Nair, M.S.,
876 Kuchipudi, S.V., Kapur, V., van Dorp, L. and Balloux, F., 2022. Transmission of SARS-
877 CoV-2 from humans to animals and potential host adaptation. Nature communications,
878 13(1), p.2988.
879
880 Taylor, L.H., Latham, S.M. and Woolhouse, M.E., 2001. Risk factors for human disease
881 emergence. Philosophical Transactions of the Royal Society of London. Series B:
882 Biological Sciences, 356(1411), pp.983-989.
883
884 Walters, B.F., Woodall, C.W., and Russell, M.B., 2016. White-tailed deer density estimates
885 across the eastern United States, 2008. Retrieved from the Data Repository for the
886 University of Minnesota, http://dx.doi.org/10.13020/D6G014.
887

888 Watanabe, T., Bartrand, T.A., Weir, M.H., Omura, T. and Haas, C.N., 2010. Development of a
889 dose-response model for SARS coronavirus. Risk Analysis: An International Journal,
890 30(7), pp.1129-1138.
891
892 Wells, W.F., 1934. On air-borne infection. Study II. Droplets and droplet nuclei. American
893 Journal of Hygiene, 20, pp.611-18.
894
895 Wilber, M.Q., Webb, C.T., Cunningham, F.L., Pedersen, K., Wan, X.F. and Pepin, K.M., 2020.
896 Inferring seasonal infection risk at population and regional scales from serology samples.
897 Ecology, 101(1), p.e02882.
898
899 Willgert, K., Didelot, X., Surendran-Nair, M., Kuchipudi, S.V., Ruden, R.M., Yon, M., Nissly,
900 R.H., Vandegrift, K.J., Nelli, R.K., Li, L. and Jayarao, B.M., 2022. Transmission history
901 of SARS-CoV-2 in humans and white-tailed deer. Scientific reports, 12(1), p.12094.
902
903 Williams, D.M., Dechen Quinn, A.C. and Porter, W.F., 2014. Informing disease models with
904 temporal and spatial contact structure among GPS-collared individuals in wild
905 populations. PLoS One, 9(1), p.e84368.
906
907 Wu, D., Wu, T., Liu, Q. and Yang, Z., 2020. The SARS-CoV-2 outbreak: what we know.
908 International journal of infectious diseases, 94, pp.44-48.
909

910 Yen, H.L., Sit, T.H., Brackman, C.J., Chuk, S.S., Gu, H., Tam, K.W., Law, P.Y., Leung, G.M.,
911 Peiris, M., Poon, L.L. and Cheng, S.M., 2022. Transmission of SARS-CoV-2 delta
912 variant (AY. 127) from pet hamsters to humans, leading to onward human-to-human
913 transmission: a case study. The Lancet, 399(10329), pp.1070-1078.

914

915 Figure Captions

916 Figure 1: Our study focuses on three stages of zoonotic spillover from humans to persistence in
917 white-tailed deer. In each stage outlined above, we describe the stage, illustrate the concept, and
918 define the metric we use to characterize each stage across multiple scenarios of deer in wild and
919 captive environments. We consider the introduction of SARS-CoV-2 into white-tailed deer
920 populations through aerosolized transmission from an infected human, quantified as the Force-
921 of-Infection (FOI_{HD}). Transmission occurs as an infected deer (orange circle) interacts with
922 susceptible deer (gray circles), transmitting SARS-CoV-2 through aerosols and fluid over the
923 course of the animal's infectious period (γ). When the individual recovers from its infection
924 (gold circle), it will have stemmed several secondary infections (orange circle), quantified as the
925 basic reproductive number ($R_0 = 4$). Depending on the magnitude of FOI_{HD} and R_0 (dashed
926 arrows), an outbreak of infections may occur across a deer population. Average prevalence in the
927 Fall season is averaged across daily values (dark line) and incidence proportion can be calculated
928 through the projected fall season (dotted line). This outbreak will either persist or fade
929 determined by the deterministic steady state of the set of ODE equations considered in this study,
930 referred to here as equilibrium (x-axis).

931

932 Figure 2: A conceptual diagram of the Susceptible-Infectious-Recovered-Susceptible (SIRS)
933 epidemiological model used for this simulation study. Objectives that focused on specific captive
934 or wild scenarios had no deer-deer fence line transmissions, preventing transmission between
935 captive or wild populations. Objective 5 focused on how fence line transmission in captive-wild
936 systems influence outbreak dynamics on both sides of the fence.

937

938 Figure 3: Box and whisker plots displaying variation in Force-of-Infection from humans-to-deer
939 (FOI), probability of at least 1 human-to-deer (HtD) transmission per 1,000 individuals during
940 the 120-day fall season, and basic reproductive numbers (R_0) across the four scenarios
941 considered in this study. Human Force-Of-Infection is log10 transformed and presented as odds
942 of HtD transmission per deer, per day. The basic reproductive number threshold between
943 unsustained and sustained transmission from deer-to-deer is indicated with a horizontal line (R_0 =
944 1). Box plots depict the minimum, first quartile, median, third quartile, and maximum, with
945 outliers depicted as single points.
946
947 Figure 4: Box and whisker plots of average prevalence and incidence proportion during the 120-
948 day fall projection in each scenario of interest, and the mean probability of SARS-CoV-2
949 persisting at the equilibrium state of the Susceptible-Infected-Recovered-Susceptible (SIRS)
950 ordinary differential equations (ODE) (with 95% confidence intervals). Box plots depict the
951 minimum, first quartile, median, third quartile, and maximum, with outliers depicted as single
952 points.
953
954 Figure 5: The relationship between human-to-deer Force-of-Infection and (A) average SARS-
955 CoV-2 prevalence, (B) persistence of SARS-CoV-2 at equilibrium in a deer population, and (C)
956 the incidence proportion during the fall is dependent on the degree of transmission from deer-to-
957 deer, quantified by the basic reproductive number (R_0), or the number of secondary infections
958 from one infected deer. Points indicate metrics for each iteration simulated, with point color and
959 shading indicating a particular scenario. Fitted lines indicate trends in the data, fitted with a log-
960 normal or logistic-regression for prevalence and persistence, respectively. Transmission

961 categories included unsustained transmission (R_0 <1), low, sustained transmission (1< $R_0 \leq 3$),
962 medium, sustained transmission (3< $R_0 \leq 5$), and high, sustained transmission ($R_0 > 5$).
963
964 Figure 6: Box and whisker plots of average prevalence and incidence proportion during the 120-
965 day fall projection and the mean probability of SARS-CoV-2 persisting at the equilibrium state
966 of the Susceptible-Infected-Recovered-Susceptible (SIRS) ordinary differential equations (ODE)
967 (with 95% confidence intervals). Plots are faceted by scenario, with variation in outbreak
968 characteristics displayed for continuous introduction from humans, and various degrees of initial,
969 single introductions with no continuous introduction from humans. Box plots depict the
970 minimum, first quartile, median, third quartile, and maximum, with outliers depicted as single
971 points.
972
973

Figures

Figure 1:

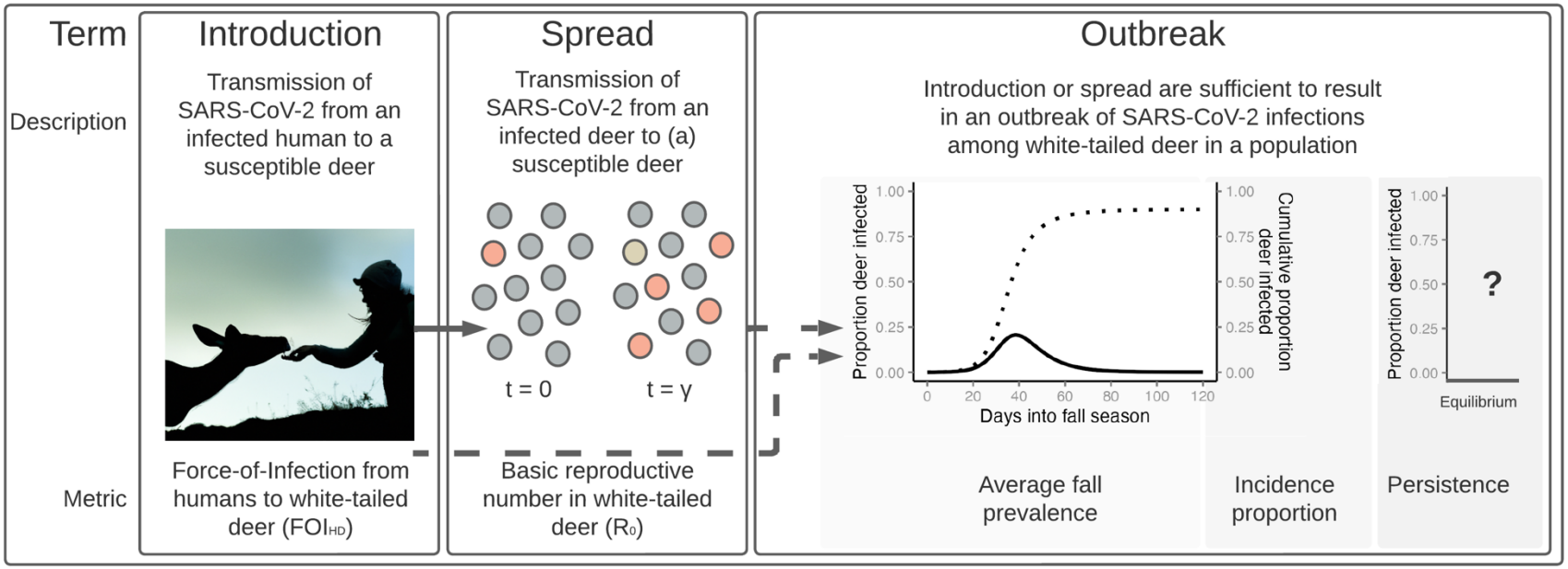

Figure 2:

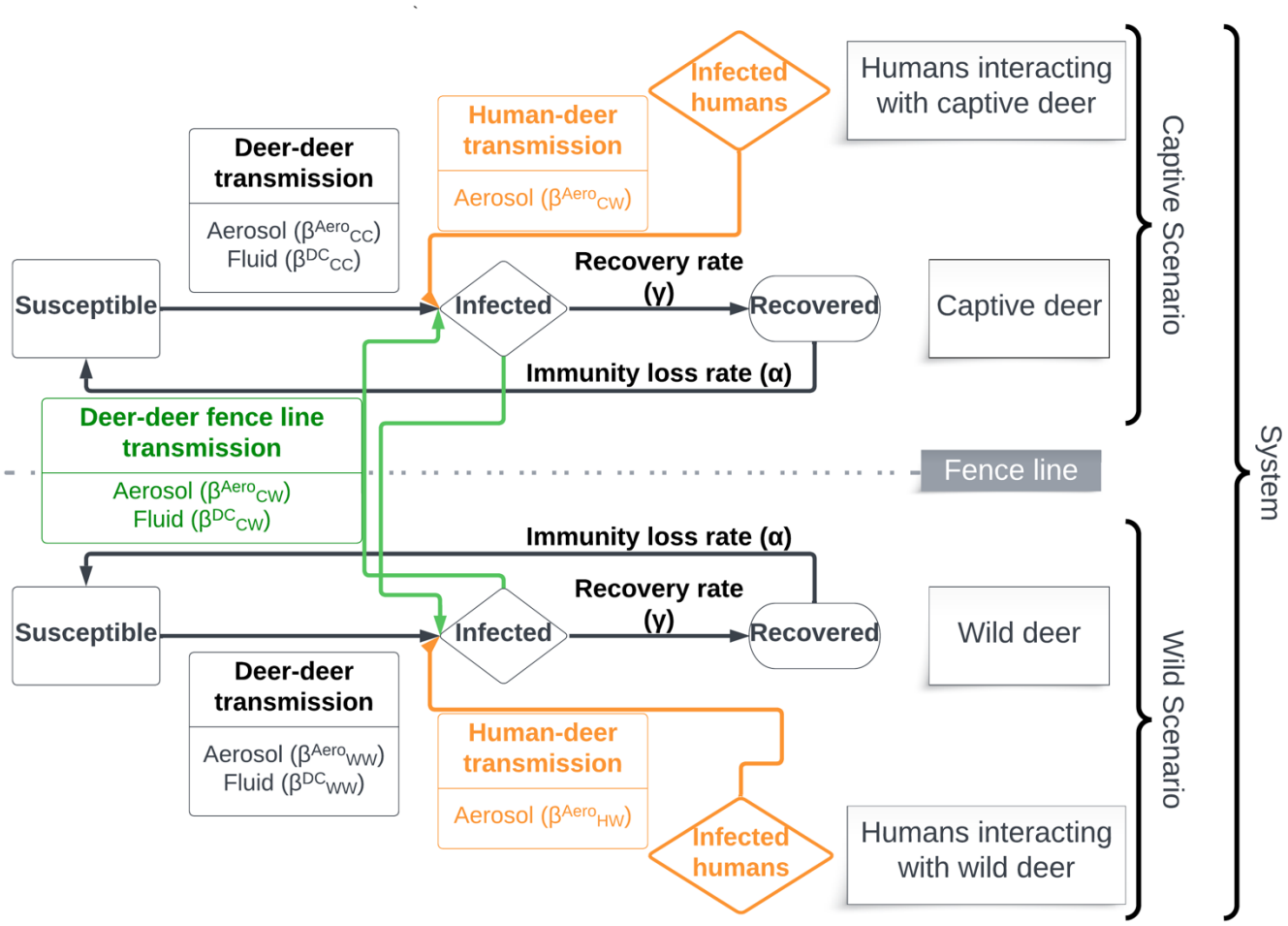
Infected humans
Humans interacting with captive deer
Human-deer transmission
Aerosol (β^{Aero}_{CW})
Deer-deer transmission
Aerosol (β^{Aero}_{CC})
Fluid (β^{DC}_{CC})
Susceptible
Infected
Recovery rate (γ)
Recovered
Captive deer
Captive Scenario
Immunity loss rate (α)
Deer-deer fence line transmission
Aerosol (β^{Aero}_{CW})
Fluid (β^{DC}_{CW})
Fence line
System
Immunity loss rate (α)
Susceptible
Infected
Recovery rate (γ)
Recovered
Wild deer
Deer-deer transmission
Aerosol (β^{Aero}_{WW})
Fluid (β^{DC}_{WW})
Human-deer transmission
Aerosol (β^{Aero}_{HW})
Infected humans
Humans interacting with wild deer
Wild Scenario

Figure 3:

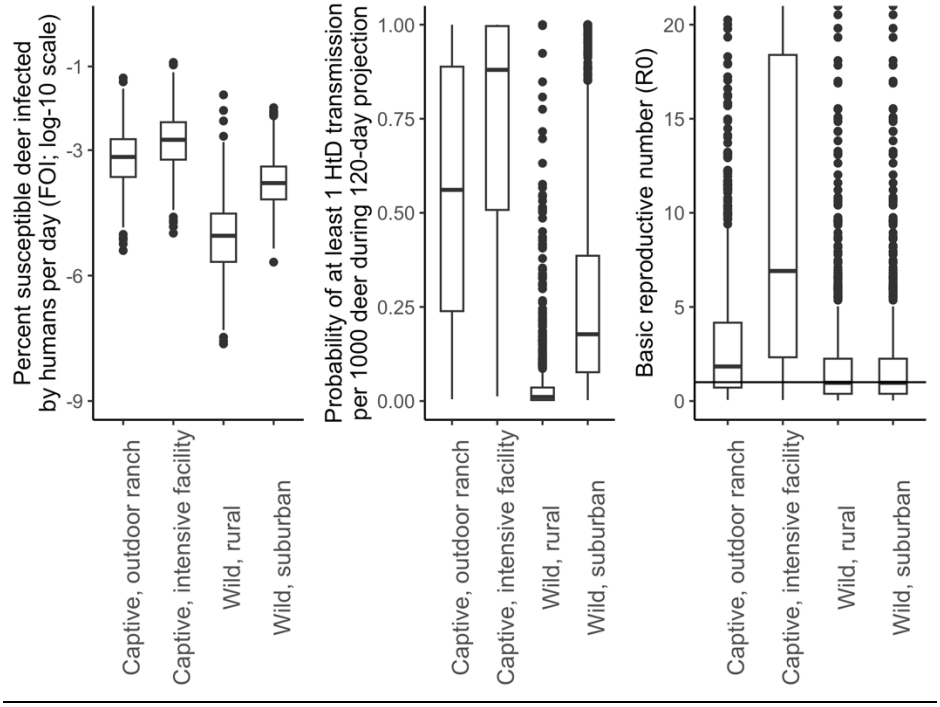

Figure 4:

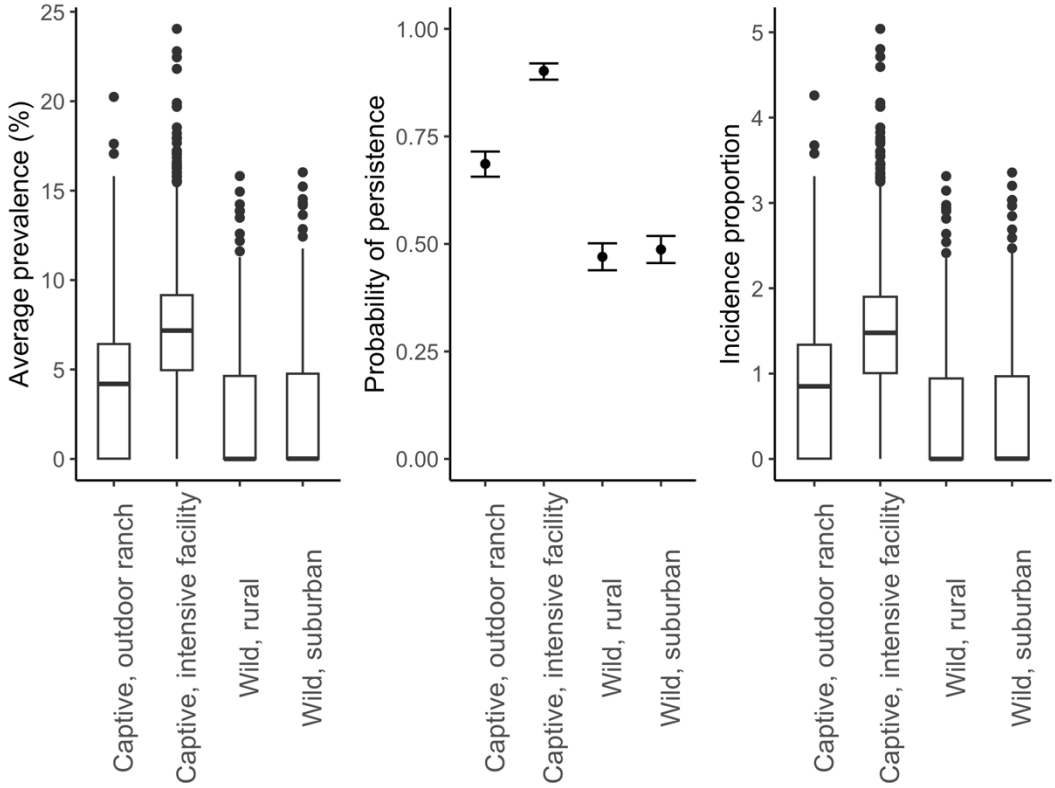

Figure 5:

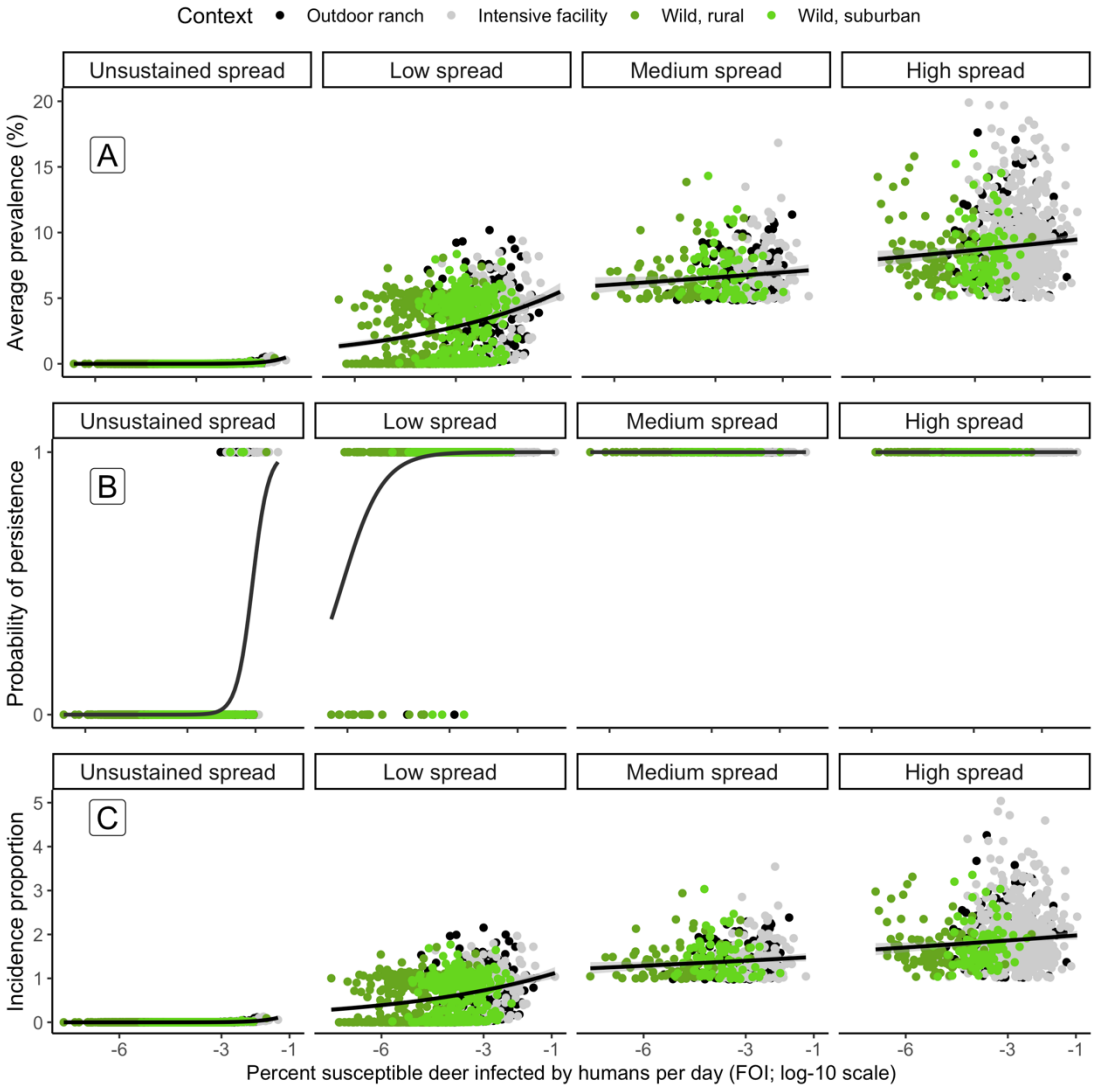

Figure 6:

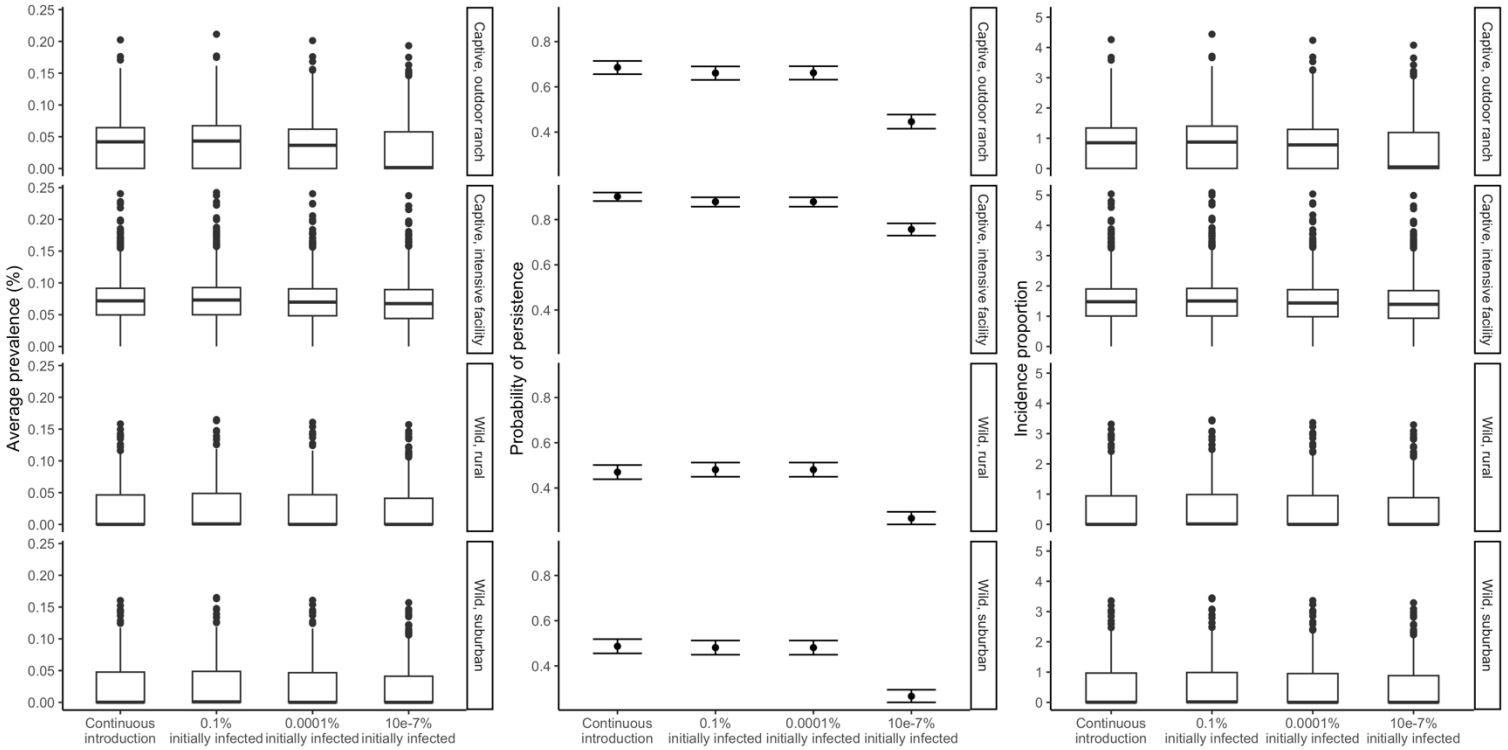
Average prevalence (%)
Probability of persistence
Incidence proportion
Captive, outdoor ranch
Captive, intensive facility
Wild, rural
Wild, suburban
Continuous introduction
0.1% initially infected
0.0001% initially infected
10e-7% initially infected

Tables

Table 1: Model parameter estimates for SARS-CoV-2 Susceptible-Infected-Recovered-Susceptible (SIRS) ordinary differential equations (ODE) for human-to-deer and deer-to-deer transmission and outbreak characteristics related to habitat or captive facility conditions, deer densities, and proximity rates with humans.. Equations refer to in-line equation numbers. Mean and standard deviation (μ and σ), along with error distribution are listed for expert-elicited estimates (Supplemental Materials). Parameters which do not apply to particular scenarios are indicated (NA).

Equations	Variable	Definition (units)	Captive		Wild		Source
			Outdoor ranch	Intensive facility	Rural	Suburban	
1, 3, 4, 6	α	Immune loss rate (day^{-1}; log-normal)	$\mu = 4.72, \sigma = 0.63$				This study, expert elicited
2, 3, 5, 6	γ	Recovery rate (day^{-1})	1/6 days				Palmer et al. 2021
1, 2, 4, 5	I_H	Human Prevalence (%)	5%				Assumed and fixed
8	κ	Proximity rate scaling adjustment (unitless)	11.35	NA	11.35	11.35	Habib et al. 2011
8	q	Proximity rate concavity scaling constant (unitless)	0.34	NA	0.34	0.34	Habib et al. 2011
8	N_w	Number of deer per unit area (A_w)	1000	NA	1000	1000	Habib et al. 2011
8	A_w	Area for intermediate density-dependence (km^2)	100 km^2	NA	100 km^2	100 km^2	Habib et al. 2011
8	$\rho_{attractant}$	Adjustment for the presence of an attractant	$\mu = 3.47$, $\sigma = 0.23$	NA	NA	NA	This study, expert elicited

		(bait, feed, etc.; log-normal)					
-	ω_{HW}	Human-deer proximity rate (events/120 days; log-normal)	$\mu = 0.57$, $\sigma = 0.95$	$\mu = 2.52$, $\sigma = 1.13$	$\mu = -1.59$, $\sigma = 1.70$	$\mu = 0.572$, $\sigma = 0.951$	This study, expert elicited
-	ω_{CC}	Deer proximity rate in captivity (events/day; log-normal)	NA	$\mu = 3.47$, $\sigma = 0.91$	NA	NA	This study, expert elicited
-	ω_{WC}	Wild-captive deer proximity rate along fences (events/day, only included for Objective 4)	0.00072 direct contacts/day / σ^{DC}				Vercauteren et al. 2007; Khouri et al. 2022
9	θ	Quanta SARS-CoV-2 dose-response in deer (1/quanta required for ID63; log-normal)	$\mu = 0.28$, $\sigma = 0.27$				This study, expert elicited
10	C_i	Conversion from SARS-CoV-2 RNA copies to quanta	0.0014 quantum/RNA copy				Mikszewski et al. 2021
10	C_v - human	Concentration of SARS-CoV-2 in human sputum (RNA copies/ml)	$\mu = 5.6$ log10 RNA copies/ml, $\sigma = 1.2$ log10				Buonanno et al. 2020
10,14	C_v - deer	Concentration of SARS-CoV-2 in deer sputum (RNA copies/ml; log-normal)	$\mu = 0.22$, $\sigma = 0.34$; proportional to C_v - human				This study, expert elicited
10	IR - human	Inhalation rate for humans, standing (m^3/hr)	0.53 m^3/hr				Mikszewski et al. 2021

10, 12	IR - deer	Inhalation rate for deer, breathing (m^3/hr)	0.85 m^3/hr				Ranslow et al. 2014
10	V_{drop}	Droplet volume concentration (speaking; ml/m^3)	0.01 ml/m3				Mikszewski et al. 2021
11	V_{air}	Volume of shared airspace with 1.5m radius (m^3)	7.07 m^3				This study, calculated
11	AER	Air exchange rate ($^{-hr}$)	4^{-hr}	1^{-hr}	4^{-hr}	4^{-hr}	Gerken et al. 2017; Bannister et al. 2023
11	s	SARS-CoV-2 settling rate ($^{-hr}$)	0.24^{-hr}				Buonanno et al. 2020
11	λ	SARS-CoV-2 inactivation rate ($^{-hr}$)	0.63^{-hr}				Buonanno et al. 2020
12	$t_{contact}$	Duration of proximity event between human and deer (minutes; log-normal)	$\mu = 1.79, \sigma = 1.15$		$\mu = -0.36, \sigma = 0.98$	$\mu = 0.432, \sigma = 0.929$	This study, expert elicited
12	$t_{contact}$	Duration of proximity event between deer (all proximity types; minutes; log-normal)	$\mu = 1.55, \sigma = 1.27$				This study, expert elicited
13	ε^{DC}	Probability of deer making direct contact (logit-normal)	$\mu = -1.46, \sigma = 0.71$				This study, expert elicited
14	k	Dose-response function for plaque-forming units (PFU required for ID63)	410				Watanabe et al. 2010

14	V_{sputum}	Volume of sputum transferred between individuals on contact (µl)	100 µl	Fixed
14	$C_{v\ -\ deer}$	Concentration of SARS-CoV-2 in deer sputum (RNA copies/ml; log-normal)	$\mu = 0.22$, $\sigma = 0.34$; proportional to C_v - human	This study, expert elicited

Table 2: Median metrics and 80% confidence intervals for simulated SARS-CoV-2 outbreaks in white-tailed deer in four scenarios. Metrics include: the proportion of susceptible deer infected by humans, per day (Force-of-Infection from humans-to-deer, FOI_{HD}); the probability of at least 1 in 1,000 deer becoming infected from a human during the fall season (probability of human-to-deer transmission, p(HTD, 1:1,000)); the number of susceptible deer infected by an infected deer (R_0); the average daily prevalence during the fall season (average prevalence); the total proportion of the population infected during the fall season (incidence proportion); and the probability of SARS-CoV-2 persisting beyond the simulated fall season (Persistence).

Scenario	FOI_{HD}	*p*(HTD, 1:1000)	R_0	Average prevalence	Incidence proportion	Persistence
Intensive facility	0.0020% (2e-4 - 0.012%)	88.0% (23.4-100.0%)	6.91 (0.84 - 43.15)	7.0% (0.001 - 11.6%)	148% (0.01 - 243%)	90% (88.2 - 92.0%)
Outdoor ranch	0.0007% (1e-4 - 0.005%)	56.1% (9.7 - 99.7%)	1.83 (0.31 - 8.83)	4.2% (0.003 - 8.8%)	85% (0.06 - 183%)	69% (65.9-71.5%)
Wild, rural	<0.0001% (0-0.0001%)	1.1% (0.1-11.2%)	0.97 (0.17-4.36)	0.001% (0-6.6%)	0.03% (0-138%)	47% (43.9 - 50.2%)
Wild, suburban	0.0002% (0-0.001%)	17.7% (3.5-66.3%)		0.01% (4e-4 - 6.9%)	0.30% (0.01 - 142%)	49% (45.6 - 51.9%)

Table 3: Increases in prevalence, incidence proportion, and persistence of SARS-CoV-2 outbreaks with simulated systems with deer in captive (outdoor ranch, intensive facility) and wild (suburban, rural) scenarios interacting across fence lines. CI = confidence interval.

System	Median increase in prevalence (80% CI)		Median proportional increase in prevalence (80% CI)		Median increase in incidence proportion (80% CI)		Mean increase in probability of persistence (80% CI)	
	Wild	Captive	Wild	Captive	Wild	Captive	Wild	Captive
Outdoor ranch and wild, suburban	0.002 (0-0.143)	0 (0-8e-4)	0.46% (0.01-104%)	0.0028 % (3e-4-0.0294)	0.044 (0-3.21)	5e-4 (0-0.016)	0.001 (1e4-0.004)	0
Intensive facility and wild, suburban	0.011 (0-0.522)	0 (0-1e-4)	11.25% (0.17-539%)	1e-04 % (0-0.003)	0.207 (2e-4-10.67)	0 (0-0.002)	0.006 (0.003-0.011)	0
Outdoor ranch and wild, rural	0.004 (0-0.557)	0 (0-8e-4)	4.47% (0.08-3094%)	9e-04 % (0-0.019)	0.081 (0-10.95)	1e-4 (0-0.016)	0.015 (0.010-0.021)	0
Intensive facility and wild, rural	0.014 (0-1.054)	0 (0-1e-4)	122.25% (0.75-19245%)	0 % (0-0.001)	0.278 (2e-4-20.42)	0 (0-0.001)	0.019 (0.014-0.029)	0